

A STUDY ON THE EFFECT OF MARTENSITE MORPHOLOGY ON MECHANICAL PROPERTIES OF HIGH-MARTENSITE DUAL-PHASE STEELS

Debdulal Das, Partha Protim Chattopadhyay,

Department of Metallurgy, Bengal Engineering College (D.U.), Howrah - 711 103

Nil Ratan Bandyopadhyay

M. N. Dastur School of Materials Science and Engineering,
Bengal Engineering College (D.U.), Howrah-711 103.

ABSTRACT

The effect of martensite morphology on the mechanical properties of high-martensite dual phase microstructure obtained by intermediate quenching (IQ) and stepquenching (SQ) of a low carbon microalloyed steel is dealt with. The IQ-treatment results in formation of fine and fibrous martensite morphology uniformly distributed in the ferrite matrix. In contrast, SQ-treatment yields blocky and banded martensite and ferrite morphology. Suitable variation of intercritical annealing temperatures adopted for both the treatments allowed the evolution of different volume fraction of martensite within a range between 0.26 to 0.71. A carefully conducted comparison of tensile results and fracture surfaces of the representative samples obtained after IQ- and SQ-treatments indicates that the morphology of martensite formed by the IQ-treatment offer better formability and toughness in the present dual-phase steels with an increased volume fraction of martensite (>0.25).

INTRODUCTION

Dual-phase steels are a class of high strength low alloy (HSLA) steels having a composite microstructure of hard martensite particles dispersed in the soft ferrite matrix. The soft ferrite matrix insures high formability and the hard martensite provides the strengthening effects [1-4]. Dual-phase steels also show continuous yielding behavior, a low yield stress, a favorable yield strength to tensile strength ratio (~ 0.5) and a high level of uniform and total elongation value with a high work-hardening coefficient [1-5]. The combination of these offer desired formability to martensite-ferrite dual-phase steels equivalent to that of steels having much lower strength, in spite of the fact that conventional HSLA steels are considered to have poor formability [3-6]. Dual-phase steels are, thus attractive materials for weight-saving application in automobile industry [1-6].

Most of the earlier studies on dual phase steel was restricted to a volume fraction of martensite below 0.25 [1-3, 7] because it was found that the ductility

and toughness decreased rapidly with increase of martensite volume fraction [2, 7, 8]. This was attributed to the formation of coarse martensite phases beyond 0.25 volume fraction. Such a restriction prompted microalloy additions to attain improved strength by the formation of fine precipitations without much affecting ductility and toughness [9-11]. It has recently been argued that the strength as well as ductility is not only determined by the content of the constituent phases, but also their morphology, size and distribution [3, 7, 12].

Review of literature indicated that work on the influence of content and morphology of martensite on the mechanical properties of dual-phase steels is limited. Kim and Thomas [13] studied the effect of microstructure in dual-phase steels on the initiation and growth of cracks under tensile loading. It was revealed that coarse martensite-ferrite duplex structure obtained by continuous annealing from the austenite region results in poor ductility and toughness with relatively high strength. On the other hand, a fine dual-phase microstructure formed by intermediate quenching gives rise to a significant improvement in both ductility and toughness without sacrificing strength [13]. Wang and Ai [6] studied the effects of martensite morphology on tensile and fatigue properties of dual-phase steels with martensite volume fraction of ~ 0.23 . They observed that among the different microstructures produced by suitable variation in heat treatment schedules, deterioration of yield and tensile strength as well as elongation occurs in the order of the fine and fibrous martensitic, blocky and netted microstructure [6]. They also showed that dual-phase steel with blocky and banded martensitic structure has better fatigue properties compared to the fibrous martensite in ferrite matrix. Among the few studies on the effect of martensite morphology on strength and ductility in high-martensite regime (>0.25) of dual-phase steels, Bag et al. [7] showed that both strength and formability are enhanced with the increase of martensite volume fraction. They achieved optimum properties at martensite volume fraction of 0.55 in case of dual-phase steels containing uniformly distributed fine fibrous martensite in ferrite matrix. In contrast, Wang and Ai [6] have reported sharp reduction in ductility against marginal increase of tensile strength with increase of martensite content for similar kind of dual-phase microstructures. A detailed study on the influence of martensite content and morphology on the mechanical properties is therefore needed for high-martensite regime of dual-phase steels and this is the aim of this work.

EXPERIMENTAL DETAILS

Predetermined charge blends were induction melted under controlled conditions. The molten metal was Cast in metal mould and the ingot homogenized at 1150°C for 2 h followed by forging to break the cast structure. The chemical composition was done in Quantovac ARL 180 and is shown in Table 1. The forged ingots were then hot rolled at 1100 °C in a laboratory scale mill (10HP) to a final thickness of 6 mm and subsequently, subjected to either intermediate quench (IQ) or step quench (SQ) heat-treatment schedules. The IQ-treatment involved a double quench operation; the specimens were first soaked at 950°C for 30 minutes, followed by quenching in water. These specimens were then annealed at different intercritical temperatures between 730-850 °C for 60 minutes and were finally quenched in

water. In the SQ-treatment, specimens were first austenitized at 950 °C for 30 minutes followed by furnace cooling to the required intercritical temperatures between 730-800 °C for 60 minutes duration before water quenching. The heat-treatment procedures are schematically represented in Fig. 1. In order to distinguish the specimens subjected to different heat-treatment schedules, they were identified with code numbers (Table 2).

Table 1 : Chemical composition of the steel in weight percent.

Elements	C	Mn	S	P	Si	Cr	Mo	V	Fe
Wt. %	0.07	1.40	0.01	0.01	1.05	0.65	0.24	0.04	Balance

Heat treated specimens were subjected to microstructural study and the volume fraction of ferrite and martensite phases were determined by image analysis using a Leica DMRX optical microscope attached with Leica Qwin image analysis software. Vickers hardness was determined using a Vickers cum Brinell hardness tester at 30 kg load. Some selected specimens were subjected to x-ray diffraction analysis to determine the amount of retained austenite in the microstructure using a PHILIPS 1710 diffractometer with Co-K α radiation and Ni filter. Tensile testing of the flat specimens, prepared according to ASTM standard (ASTM: Vol.03.01 :E8M-96), was conducted at room temperature in a computer controlled Instron 4204 machine using a cross head velocity of 0.5 mm/min without extensometer. Values of yield stress, ultimate tensile stress, uniform and total elongation and tensile toughness were obtained. Fracture surfaces of tensile specimens were analyzed using a JEOL, JSM 5200 Scanning Electron Microscope.

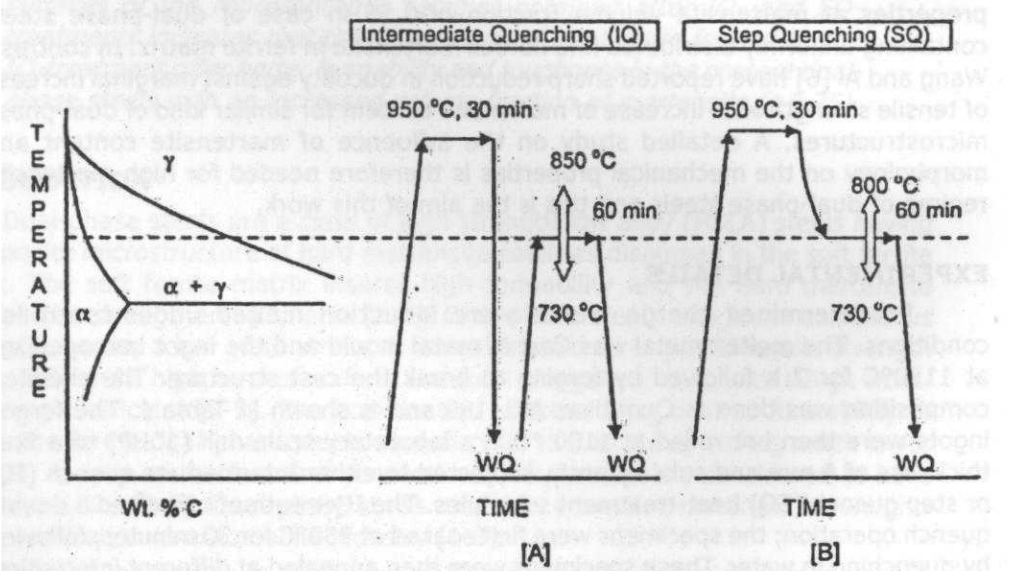


Fig. 1 : Schematic representation of heat treatment schedules for [A] IQ and [B] SQ-treatments.

Table2 : Heat-treatment schedules for achieving various dual-phase microstructures.

Type of Heat-treatment	Specimen code	Austenitizing treatment at 950°C for 30 min, followed by -	Intercritical annealing temperature (°C) for 60 min followed by water quenching
Intermediate quenching (IQ-)	IQ-730	Water quenching	730
	IQ-750		750
	IQ-775		775
	IQ-800		800
	IQ-825		825
	IQ-850		850
Step quenching (SQ-)	SQ-730	Furnace cooling	730
	SQ-750		750
	SQ-775		775
	SQ-800		800

RESULTS AND DISCUSSION

Microstructure

Fig. 2 and Fig. 3 present some selected optical micrographs of IQ-treated and SQ-treated specimens, respectively. The metallographic samples were etched with 5% nital solution to reveal the martensite phases as 'dark' regions and the ferrite phases as 'white' regions in the micrographs. The microstructures were subjected to appropriate image analysis procedure with an aim to carry out measurement of volume fraction of martensite (V_M). Fig. 4 shows the variation of V_M as a function of intercritical annealing temperatures (T_{ICA}) for both IQ- and SQ-treatments.

It is evident from figs. 2 and 3 that both IQ- and SQ-treatments result into ferrite-martensite dual-phase microstructures with remarkable variation in the morphology and distribution of martensite phase. The ferrite-martensite composite microstructure in SQ-specimens exhibits a banded morphology with non-uniform distribution of the blocky regions of the concerned phases (Fig. 3). In contrast, IQ-specimens exhibit fine and fibrous nature of predominantly lath martensites dispersed uniformly in the ferrite matrix (Fig. 2). The variation of morphology and distribution of the constituent phases for the chosen heat-treatment schedules are comparable to those reported earlier in the literature [6, 7]. The observed difference in the evolution of microstructure in the IQ- and SQ-specimens after intercritical annealing is apparently due to the differences in the microstructural state of the samples before they are subjected to the intercritical annealing treatment (Fig. 1): It may be noted that in case of IQ-specimens the microstructures are completely martensitic prior to intercritical annealing, whereas the microstructures of SQ-specimens are completely austenitic before intercritical annealing (Fig 1). Therefore, during annealing in the two-phase region, both ferrite and austenite evolve from the initial

martensite phase in case of IQ-treatment, whereas only a part of austenite transform to ferrite in case of SQ-treatment.

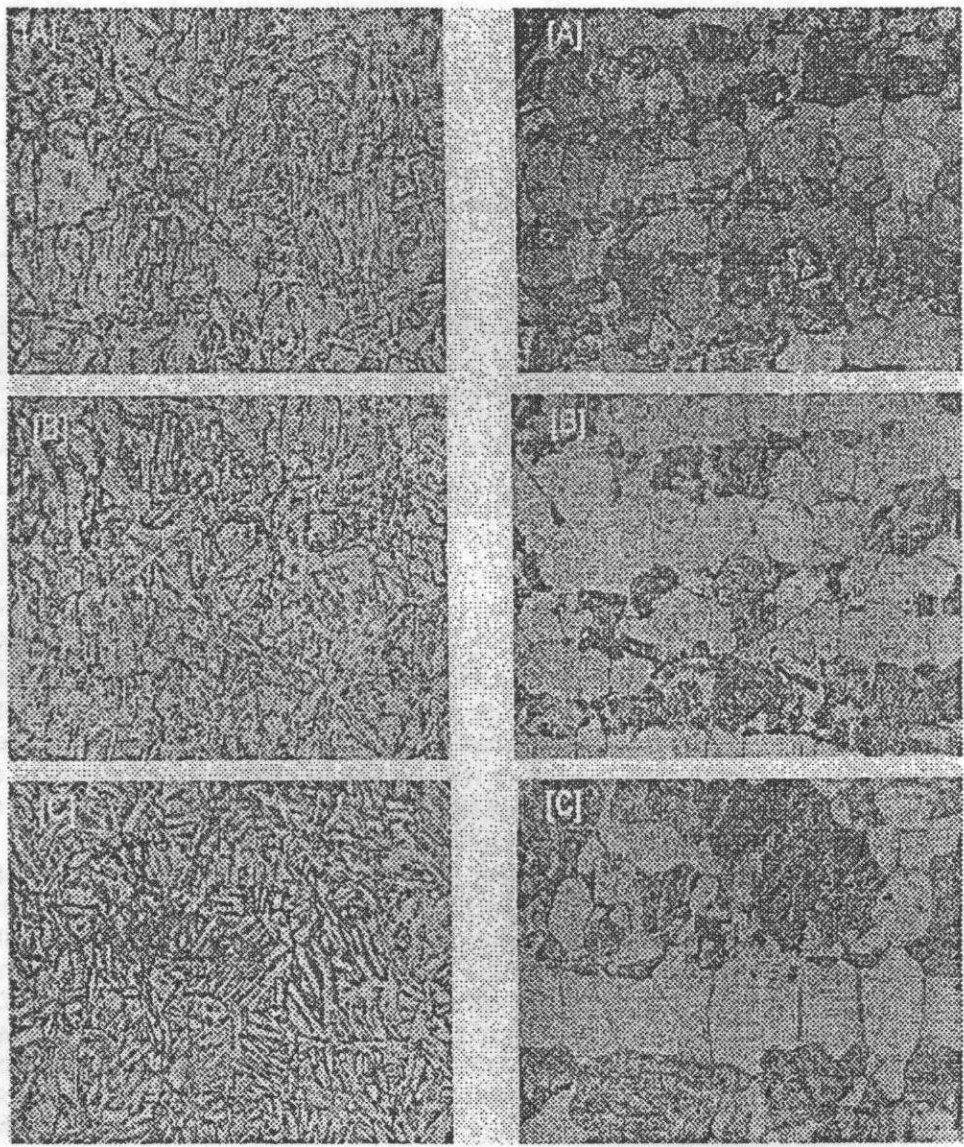


Fig. 2 : Optical micrographs of IQ-treated dual-phase steels showing the distribution of fine, fibrous martensite (black) and ferrite (white). Micrographs [A], [B] and [C] correspond to the microstructures obtained with T_{ICA} at 730, 775 and 800 °C, respectively at 500X

Fig. 3 : Optical micrographs of SQ-treated dual-phase steels showing the banded microstructure with blocky martensite (black) and ferrite (white). Micrographs [A], [B] and [C] correspond to the microstructures obtained with T_{ICA} at 730, 775 and 800 °C, respectively at 500X.

The morphology and dispersion of the martensite phase in the IQ-treated specimens depend on the process of reversion of austenite from the initial tempered martensite. The nucleation of austenite and ferrite phases from the tempered martensite can occur at different sites such as (i) the prior austenite grain boundaries, (ii) the carbide precipitates on prior austenite grain boundaries, (iii) the spheroids in ferrite, and (iv) the fine carbides particles formed on the prior martensite plate/lath boundaries [7]. Therefore, during intercritical annealing of IQ-specimens, both ferrite and austenite phases preferentially form in the above mentioned nucleating sites and grow along those locations. The austenite regions transform to martensites during subsequent water quenching. The availability of finer and well-dispersed nucleating sites in large population causes fine and fibrous morphology of the well dispersed martensite in the final dual-phase microstructure. On the other hand, the morphology of the ferrite and martensite regions in the SQ-specimens depends on the formation of ferrite phase only in the austenite matrix during cooling from completely austenitic region to two-phase region (Fig. 1B). The nucleation of ferrite starts at austenite grain boundaries, and these nuclei grow inside the austenite matrix results in distinct regions of ferrite and austenite. On subsequent water quenching from two-phase region the untransformed austenitic regions transform to martensites. The resultant martensite can have both plate and lath morphology, the later being predominant in specimens treated at lower T_{ICA} . The difference in the genesis of austenite in the two-phase regions, thus, lead to the varied morphologies of martensite in the dual-phase micro structures processed via the IQ- and SQ-routes. The problem of banding does not appear in the IQ-treated samples, because of the existence of a large number of different types of nucleation sites for austenite and ferrite phases in the initial martensitic microstructure.

Fig. 4 reveals that the V_M increases with increase of T_{ICA} for both the present treatments due to the fact that volume fraction of austenite in equilibrium with ferrite in the two-phase region increases with increase of T_{ICA} . For example, the V_M increased from 0.38 to 0.69 for the increase of T_{ICA} from 750 to 825 °C for IQ-specimens. On the other hand, for SQ-specimens, V_M varied from 0.26 to 0.64 when T_{ICA} increased from 730 to 800 °C. At any given T_{ICA} , V_M in the SQ-specimens is only 1-3% higher than the IQ-specimens (Fig. 4). The comparable value of V_M in the IQ- and SQ-specimens apparently indicates that intercritical annealing for 60 minutes allowed the ferrite and austenite to attain the equilibrium irrespective of the type of initial microstructures. However, the size of lath martensite was found to be larger with increase of V_M in IQ-specimens as shown in Figs. 2(A), (B) and (C). In SQ-specimens, the sizes of martensite blocks and ferrite grain size increase with increase in T_{ICA} as a result of grain coarsening of austenite at higher T_{ICA} [Figs. 3 (A), (B) and (C)].

It is important to note that no visible carbide or nitride precipitates are present in the optical micrographs as shown in Figs. 2 and 3. Even in the case of any probable presence of carbides or nitrides, too small in size to be identified in the optical microstructure, it will not be unrealistic to postulate that their volume fractions are inadequate to influence the mechanical properties of the present dual-phase steels due to reasonably low carbon content in the steel (Table 1). However, presence of 1.4 wt. % Mn in the steel prompts to predict the presence of some amount of

retained austenite in the microstructure. With an aim to examine the presence of any significant amount of austenite in the microstructure, x-ray diffraction analysis of some selected samples were carried out. However, absence of any notable peak concerned with austenite in the x-ray line profiles of both IQ- and SQ-specimens has allowed to rule out any significant presence of retained austenite in the microstructure. In this regard, higher applied cooling rate from the two-phase region (i.e., water quenching) and higher hardenability of the present steel caused by the presence of elements like Cr, V and Mo, may be held responsible for the absence of retained austenite in the x-ray diffraction profile.

Mechanical Properties

Fig. 5 summarizes the results of Vicker's hardness testing carried out at a load of 30 kg for all IQ- and SQ-specimens. It is evident that for both the treatments, the hardness increases with T_{ICA} (Fig. 5), due to increase in the volume fraction of the hard phase, i.e., martensite, with increase of T_{ICA} (Fig. 4). However, at a given T_{ICA} (i.e., nearly same V_M), IQ-specimens reveal significantly higher hardness values in comparison to their SQ-counterparts as shown in Fig. 5. For example, IQ-specimen shows the hardness value of 202 VHN as compared to 170 VHN of SQ-specimen at $T_{ICA} = 800^\circ\text{C}$. The higher hardness of IQ-specimens may be attributed to the fine and uniform distribution of martensite phase in the microstructure, where as blocky and banded nature of ferrite and martensite phases in SQ-specimens perhaps results in lower hardness value.

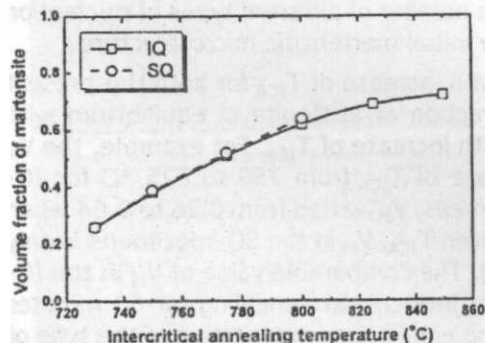


Fig. 4 : Volume fraction of martensite as a function of intercritical annealing temperature for IQ- and SQ-treated dual-phase steels.

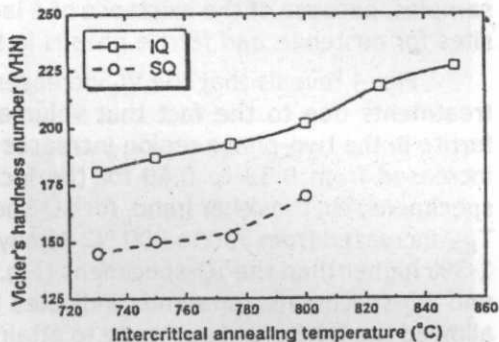


Fig. 5 : Vicker's hardness number as a function of intercritical annealing temperature for IQ- and SQ-treated dual-phase steels.

The variation in the yield strength and ultimate tensile strength of IQ- and SQ-steels with V_M are shown in Fig. 6. The values of the uniform elongation and the total elongation as a function of V_M are given in Fig. 7. It is revealed in Fig. 6, that the yield strength as well as tensile strength increases with increasing V_M in both IQ- and SQ-specimens. However, yield strength as well as tensile strength shows greater dependence on V_M in case of SQ-specimens as compared to IQ-specimens.

In case of IQ-steels, the yield strength and tensile strength increase gradually with V_M up to a value of 0.6. For V_M higher than 0.6, yield strength increases sharply with further increase of V_M , while tensile strength continue to increase gradually followed by a slight drop after $V_M > 0.70$. The ductility, as characterized by uniform and total elongation decreases with increasing V_M for both IQ- and SQ-treated steels. However, at any given V_M , IQ-specimen shows significantly higher ductility compared to SQ-specimen (Fig. 7). It may be noted that while the uniform and total elongation decreasing almost linearly with V_M for SQ-steels, variation of the same as a function of V_M for IQ-steels is negligible for $V_M \leq 0.5$. Thus, the results shown in Fig. 7, clearly demonstrate that the dual-phase steels containing coarse (as in IQ-steels with higher V_M) or banded (as in all the SQ-steels examined) martensite structures will provide the ductility inferior to those containing finely dispersed martensite coarse (as in IQ-steels with lower V_M). It is interesting to note that the IQ-steels have lower yield strength and nearly same or marginally higher tensile strength but significantly higher ductility when compared with the SQ-steels containing comparable V_M . This observation is in good agreement with previous reports [6, 7, 12, 14].

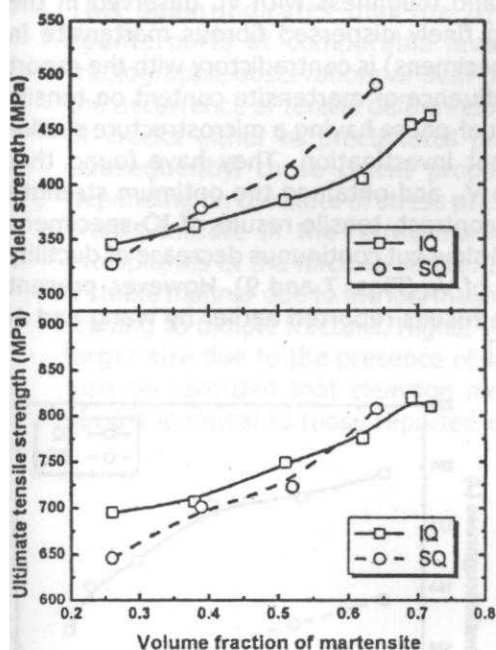


Fig. 6: Variation of yield strength and ultimate tensile strength as a function of volume fraction of martensite for IQ- and SQ-treated dual-phase steels.

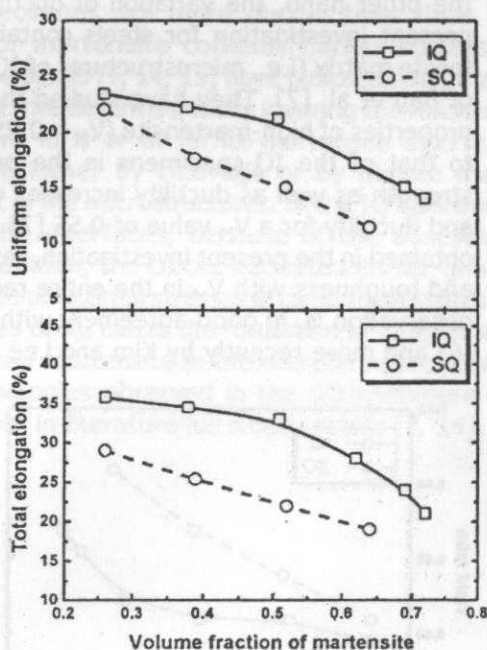


Fig. 7: Variation of uniform elongation and total elongation as a function of volume fraction of martensite for IQ- and SQ-treated dual-phase steels.

Fig. 8 shows the variation of yield ratio, i.e., yield strength to tensile strength as a function of V_M . It is generally recommended that for dual-phase steel, the yield ratio should be low and its value close to 0.5 is considered to be ideal [3]. In the present steel the IQ-specimens have yielded the values of yield ratio close to the ideal value (i.e., ~ 0.5) for $V_M \leq 0.6$ without showing any notable dependence on V_M (Fig. 8). In contrast, for SQ-specimens the yield ratio increases sharply with V_M over the entire range of V_M in the present investigation (Fig. 8). At any comparable V_M in the present dual phase steel, the IQ-specimens have lower yield ratio than the SQ-specimens indicating the microstructure evolution in the case of IQ-specimens are favorable than the SQ-specimens for the purpose of obtaining better mechanical properties. Tensile toughness values as measured here from the area under the stress-strain diagrams are plotted as a function of V_M in Fig. 9. It is interesting to note that the tensile toughness is higher for IQ-steels than SQ-steels at comparable V_M . This again substantiates the fact that the finely dispersed fibrous lath martensite in the ferrite matrix obtained in the case of IQ-specimens should be preferred over the blocky and banded nature of ferrite and martensite phases in the SQ-specimens for the production of dual-phase steels with improved toughness. This observation is consistent with the earlier reports by Wang and Al [6] and Kim and Lee [14]. On the other hand, the variation of ductility and toughness with V_M observed in the present investigation for steels containing finely dispersed fibrous martensite in ferrite matrix (i.e., microstructures of IQ-specimens) is contradictory with the report of Bag et al. [7]. They have studied the influence of martensite content on tensile properties of high-martensite ($V_M > 0.25$) dual-phase having a microstructure similar to that of the IQ-specimens in the present investigation. They have found that strength as well as ductility increases with V_M and obtained the optimum strength and ductility for a V_M value of 0.55 [7]. In contrast, tensile results of IQ-specimens obtained in the present investigation, reveal slow but continuous decrease of ductility and toughness with V_M in the entire range of V_M (Figs. 7 and 9). However, present observation is, in good agreement with the results reported earlier by Wang and Al [6] and more recently by Kim and Lee [14].

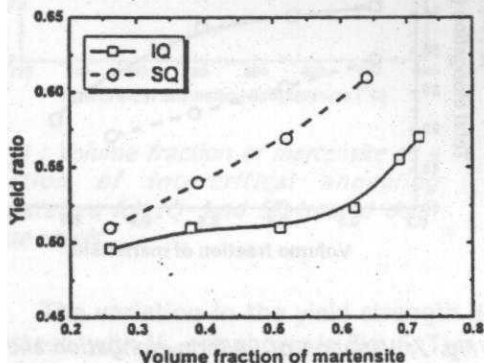


Fig. 8 : Yield ratio as a function of volume fraction of martensite for IQ- and SQ-treated dual-phase steels.

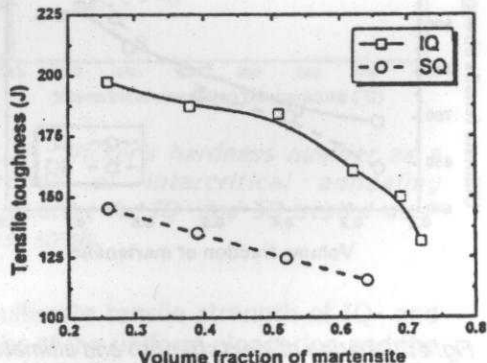


Fig. 9 : Tensile toughness as a function of volume fraction of martensite for IQ and SQ-treated dual-phase steels

Factography

Scanning electron micrographs of fractured tensile surface of IQ-specimens containing a V_M value of 0.26, 0.51 and 0.62 are shown in Figs. 10 (A), (B) and (C), respectively. These factographs reveal the presence of dimples, indicating the occurrence of typical ductile mode of fracture due to the higher ductility yielded by those specimens (Fig. 7). Closer observation of the factographs further reveal that the size of the dimples increases with V_M , perhaps due to formation of coarse martensite at higher value of V_M (Fig. 7). This prediction is consistent with the measured values of uniform and total elongation, which decrease with higher values of V_M . Figures 11 (A), (B) and (C) represent the fractograph of tensile surface of SQ-specimens containing V_M of 0.26, 0.52 and 0.64, respectively. While predominantly ductile mode of fracture with large dimple size was observed for SQ-specimen with lower (Fig. 11A), quasi-cleavage mode of fracture is dominant in the SQ-specimens with higher V_M as shown in Figs. 11(B) and (C). This change of fracture morphologies with V_M is in accordance with the observations that the ductility reduces sharply with V_M for SQ-specimens [3, 7, 14]. At a given value of V_M (say, ~ 0.52), fracture surface of IQ-specimens show dimple fracture, whereas SQ-specimens exhibit quasi-cleavage fracture with predominantly cleavage nature (Fig. 10B) vis-a-vis (Fig. 11B). This again indicates that the IQ-specimens are more ductile than their SQ-counterparts at comparable levels of martensite content. Earlier studies on fractographic observations of dual-phase steels [7, 14, 15] have indicated that during the occurrence of tensile deformation, ferrite deforms initially favoring the nucleation of cracks either at precipitates present in it or at ferrite-martensite interfaces. Subsequently, these cracks propagate either by cleavage or by dimple mode, depending on the state of stress present in the microstructures. In the IQ-specimens, cracks initiate in the ferrite-martensite interfaces, because of the absence of precipitates in the microstructure. In addition, the cracks nucleated earlier grow in a stable manner due to the low magnitude of internal stresses in these microstructures leading to dimple fracture. Higher values of V_M cause the formation of dimples with larger size due to the presence of coarser martensite in the microstructure. It may also be recorded that cleavage morphologies observed in the SQ-specimens are almost identical to those reported earlier in literature for similar steels [7, 14].

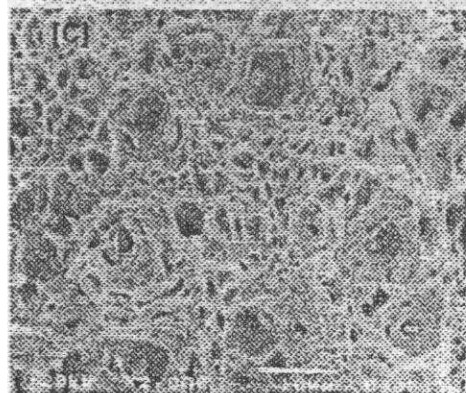
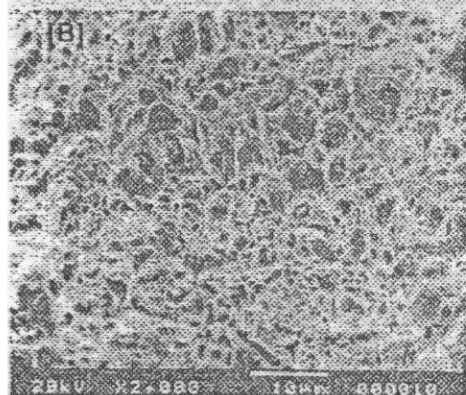
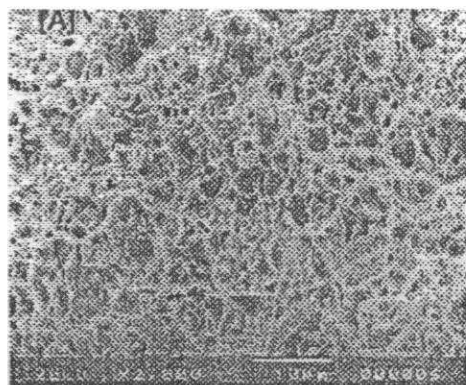


Fig. 10 : Scanning electron factographs of IQ-treated dual-phase steels. Factographs [A], [B] and [C] correspond to the microstructures obtained with τ_{ca} at 730, 775 and 800 °C, respectively.

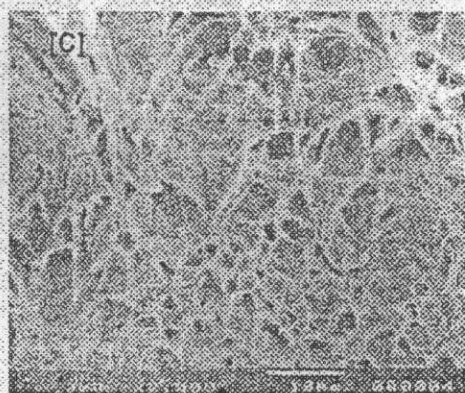
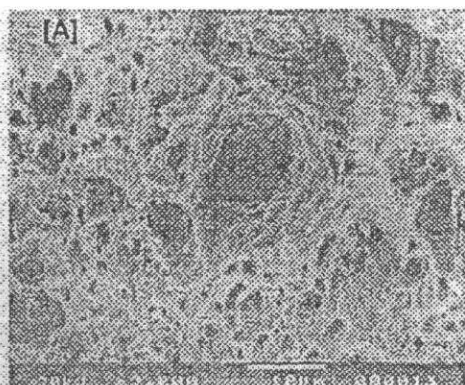


Fig. 11 : Scanning electron factographs of SQ-treated dual-phase steels. Factographs [A], [B] and [C] correspond to the microstructures obtained with τ_{ca} at 730, 775 and 800 °C, respectively.

CONCLUSIONS

1. The intermediate quenching results in uniform distribution of fine and fibrous martensite in the ferrite matrix, whereas step quenching yields blocky and banded ferrite and martensite phases. The difference in microstructural state before intercritical annealing may be held responsible for the observed differences in the final microstructures.
2. For comparable martensite content, intermediate quenching yield better strength, ductility, toughness and a nearly ideal yield ratio due to formation of a favorable morphology of the dual-phase microstructure unlike the step-quenching treatment.
3. Increase in martensite volume fraction causes increase in yield and tensile strength for both the treatments. However, the rate of reduction of ductility and toughness with martensite content is more prominent in case of step quenching compared to intermediate quenching treatment.
4. Analysis of fracture surfaces shows occurrence of dimple fracture in the IQ specimens, in contrast to the quasi-cleavage mode of fracture in the SQ-specimens.
5. Intermediate quenching treatment may be recommended as the suitable route for manufacturing high strength dual-phase steels with higher martensite volume fraction (i.e., > 0.25) without any serious detriment to the formability and toughness due to formation of favorable morphology and distribution of martensite.
6. The intermediate quenching of the present dual phase steel yields the most favorable combination of properties for a martensite volume fraction close to 0.5.

REFERENCES

1. Structure and Properties of Dual-Phase Steels, Kot, R. A. and Morris, J. W., (eds.) AIME, New York, NY, 1979.
2. Fundamental of Dual-Phase Steels, Kot, R. A. and Bramfitt, B. L., (eds.) AIME, New York, NY, 1981.
3. Speich, G.R., Physical Metallurgy Of Dual Phase Steels in Fundamentals of Dual Phase Steel, The Metallurgical Society, (1981) 1.
4. Llewellyn, D.T. and Hillis, D.J., Ironmaking and Steelmaking, 23 (1996) 471.
5. Hills, D.J., Llewellyn, D.T. and Evans, P.J., Ironmaking and Steelmaking, 25 (1998) 47.
6. Wang, Z. G. and Al, S.H., ISIJInt., 39 (1999) 74.
7. Bag, A. A., Ray, K. K. and Dwarakadasa, E. S., Metall. Trans., 30A (1999) 1193. 16
8. Kang, S. and Kwon, H, Metall. Trans., 18A (1987) 1573.
9. Ghosh, S.K, Das, D. and Chattopadhyay, P.P., IE(I) Journal-MM, 82 (2001) 50.
10. Terao, N. and Baugnet, J. Mat. Sci., 25 (1990) 848.
11. Soto, R., et al., Acta Mater., 47 (1999) 3475.
12. Bag, A. A. Ray, K. K. and Dwarakadasa, E. S., Metall. Trans., 32A (2001) 2207.
13. Kim, N. J. and Thomas, G., Metall. Trans., 12A (1981) 483.
14. Kim, S. and Lee S., Metall. Trans., 31A (2000) 1755.
15. Devis, R. G., Metall. Trans., 9A(1978) 671; 10A (1979) 113.